PAIN®

Inhibition of transient receptor potential vanilloid 1 and transient receptor potential ankyrin 1 by mosquito and mouse saliva

Sandra Derouiche[a,b,c], Tianbang Li[a,b], Yuya Sakai[d], Daisuke Uta[e], Seiji Aoyagi[d], Makoto Tominaga[a,b,c,*]

Abstract

Arthropods are the largest group of living organisms, and among them, mosquitoes spread parasites and viruses causing deadly diseases. They can easily spread these pathogens because of their painless skin piercing. Although the lack of pain is mainly due to the thinness of their fascicle, it is possible that mosquito saliva, which is discharged during their piercing, might also contribute to it. If mosquito saliva contains antinociceptive substances, it should act on the sensory neurons innervating the epidermis where there are several ion channels that can detect noxious stimuli, such as the transient receptor potential (TRP) channels. We found that mosquito head homogenates and mouse saliva inhibit TRP vanilloid 1 (TRPV1) and TRP ankyrin 1 (TRPA1) channels, either heterologously expressed in HEK293T cells or endogenously expressed in native mouse sensory neurons. Among the different substances contained in mosquito head homogenates or mouse saliva, we have also identified sialorphin as a candidate antinociceptive peptide because it showed similar inhibition effects on TRPV1 and TRPA1. Finally, we confirmed the antinociceptive effects of mosquito head homogenates, mouse saliva, and sialorphin in vivo by observing decreased pain-related behaviors in mice coinjected with these substances. Similar inhibitory effects of mosquito head homogenates and mouse saliva on TRPV1 and TRPA1 suggest that the antinociceptive effects of saliva are universal, which could explain why many animals including humans often lick their wounds. These findings would lead to the development of novel and safe antinociceptive agents.

Keywords: Painless, Mosquito, Saliva, TRPV1, TRPA1

1. Introduction

Arthropods are the largest group of living organisms. They attack other organisms by biting, stinging, piercing, and sucking. Among the various arthropods that affect human health by feeding on living hosts, piercing by mosquitoes spreads parasites and viruses, some of which have been reported to cause the highest number of deaths annually, including malaria, dengue fever, and West Nile fever[17] (**Fig. 1A**). The mosquito fascicle, which is composed of 6 stylets, is approximately 70 μm in diameter, being far thinner than commercial medical needles of which diameter are usually over several hundred micro meter.[15] One of the reasons why mosquito piercings are painless is the thinness of their fascicle, and the potential for fascicles to avoid pain receptors (free nerve endings) becomes higher as they become thinner. Over their long process of evolution, mosquitoes have adapted by dividing the needle into a fascicle of 6 stylets,[5] and mosquitoes can move these stylets with great dexterity, which also contributes to the painless piercing.[2] Saliva is discharged through cooperative movement of the stylets even before they reach the blood supply. Once they reach the blood source, the cooperative motion of the stylets ceases and saliva is frequently discharged as they suck the blood.[6] Although the microneedle properties of the fascicle are currently believed to explain the painless piercings by mosquitoes, it is possible that mosquito saliva might also contribute to this lack of pain. Mosquito saliva is a complex of proteins; many of which have unknown functions but some allow the mosquito to acquire a blood meal from its host by circumventing vasoconstriction, platelet aggregation, coagulation, and inflammation or hemostasis.[14] Mosquito saliva also contains proteins that are immunogenic to humans and cause allergic responses, as we often experience. Given these properties, we hypothesized that mosquito saliva also contains antinociceptive substances that contribute to their painless piercings.

Under normal conditions, mosquito saliva should act on the sensory neurons innervating the epidermis. In these sensory nerve endings, there are several ion channels expressed that can detect noxious stimuli, including transient receptor potential
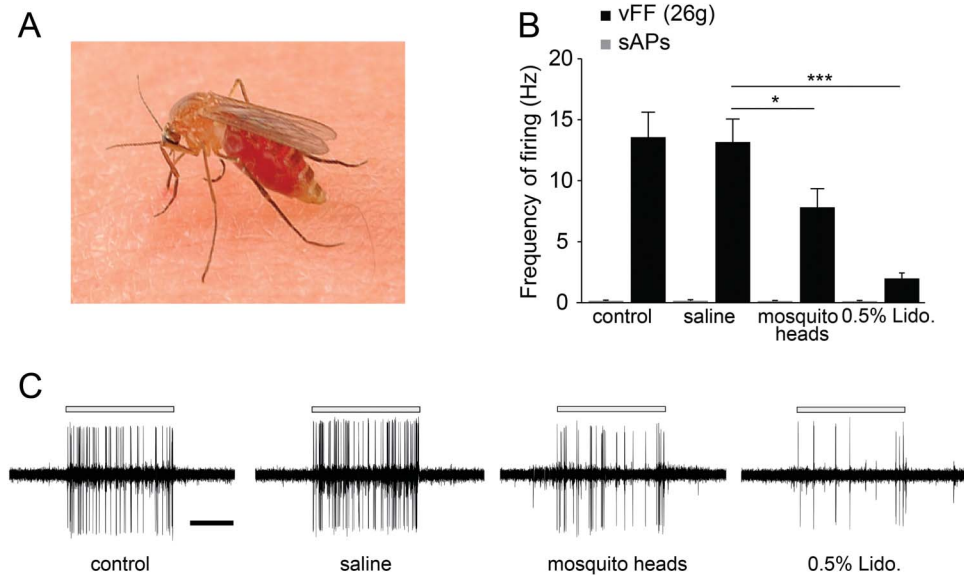
Figure 1. Effect of mosquito head homogenates on rat spinal neurons activity. (A) Photograph of *Culex pipiens pallens* on the human skin. (B) Inhibition of von Frey filament (vFF)-evoked neuronal firing frequency in rat spinal dorsal horn neurons by 0.5% lidocaine (Lido) or a 10-fold dilution of mosquito (*C. pipiens pallens*) head homogenates. *$P < 0.05$, ***$P < 0.001$ by one-way ANOVA followed by a Bonferroni post hoc test (n = 10 rats for each group). (C) Representative recordings of neuronal firing as analyzed in (B). A black scale bar indicates 4 seconds. ANOVA, analysis of variance; sAPs, spontaneous action potentials.

(TRP) channels. These ion channels constitute a family of polymodal cell sensors, and among those, TRP vanilloid 1 (TRPV1) and TRP ankyrin 1 (TRPA1) were reported to be activated by mechanical stimuli, which is supposed to function during mosquito piercing, in addition to noxious chemicals or high temperature in HEK293T cells.[3,7,8] Therefore, we investigated the antinociceptive properties of mosquito head homogenates and mouse saliva at both in vitro and in vivo levels, by focusing on TRPV1 and TRPA1 channels.

2. Methods

2.1. Animals

Adult mosquito of *Culex pipiens pallens* were from Research and Development Laboratory, Dainihon Jochugiku Co, Ltd (Osaka, Japan). Mouse experiments were conducted with 6- to 8-week-old C57BL/6NCr male mice. All the animal experiments were performed in accordance with the guidelines of the National Institute for Physiological Sciences, University of Toyama, and the National Institutes of Health (NIH).

2.2. Chemicals

Capsaicin, citronellal, allyl isothiocyanate (AITC), and carbachol were purchased from Sigma-Aldrich (St. Louis, MO). Rat sialorphin was purchased from Phoenix Pharmaceuticals, Inc (Burlingame, CA).

2.3. Isolation of mosquito heads

We decided to use mosquito head homogenates instead of taking saliva from mosquito salivary glands because we needed large amounts of mosquito saliva for various experiments. After anesthesia with diethyl ether, the mosquito heads with salivary glands were excised from 50 female mosquitoes, followed by homogenization in 800 μL of 0.9% saline and centrifugation at 15,000 rpm for 15 minutes. The supernatant solution of 700 μL

obtained here was used as the mosquito head homogenate solution and stored at −20°C until use. If a larger amount was necessary, the process mentioned above was repeated for additional 50 mosquitoes.

2.4. Isolation of mouse saliva

In brief, mice were maintained anesthetized with isoflurane. Mouse's neck skin was surgically removed, and their submandibular glands were exposed. Stimulation of salivation was elicited by the injection of the muscarinic agonist carbachol (20 μL, 50 μM) into each submandibular gland. Saliva was then directly collected by pipetting from the mice mouth and stored at −20°C until use.

2.5. Cell culture

The human embryonic kidney 293T (HEK293T) cells were cultured in Dulbecco's modified Eagle medium (Wako, Osaka, Japan) supplemented with 10% fetal bovine serum (BioWest Riverside, MO), penicillin-streptomycin (50 mg/mL and 50 units/mL, respectively, Gibco), and GlutaMAX (2 mM, Gibco, Waltham, MA). For transient transfection of HEK293T cells, 1 μg of plasmid DNA in pcDNA3.1 (+) and 0.1 μg of pGreen-Lantern 1 vector were transfected into HEK293T cells using Lipofectamine reagent and Plus reagent (Invitrogen Corp., Carlsbad, CA). In the case of transfection for calcium imaging, 0.1 μg of pCMV-DsRed vector was transfected instead of pGreen-Lantern 1 vector. All these components were dissolved in Opti-MEM medium (1X, Gibco). After incubation for 3 to 4 hours, HEK293T cells were reseeded on 12-mm coverslips (Matsunami, Kishiwada, Japan) and further incubated at 33°C in 5% CO_2.

2.6. In vivo *extracellular recording in rat*

The methods used for the in vivo patch-clamp recording of substantia gelatinosa neurons were similar to those previously

described.[19] In brief, the rats were anesthetized with urethane (1.5 g/kg, i.p.), which produces a long-lasting steady level of anesthesia and does not require the administration of additional doses except in few cases. A thoracolumbar laminectomy was performed to expose the L1 to L6 vertebrae, followed by placing the animal in a stereotaxic apparatus. Next, the dura was removed and the arachnoid membrane was cut to create a large window for a tungsten microelectrode. The surface of the spinal cord was irrigated with Krebs solution equilibrated with 95% O_2 and 5% CO_2 (10-15 mL/minute) and containing 117 mM NaCl, 3.6 mM KCl, 2.5 mM $CaCl_2$, 1.2 mM $MgCl_2$, 1.2 mM NaH_2PO_4, 11 mM glucose, and 25 mM $NaHCO_3$ (pH = 7.4) at 37 ± 1°C. Extracellular single-unit recordings of superficial dorsal horn (laminae I and II) neurons were performed as follows. Recordings were obtained from the superficial dorsal horn neurons at a depth of 20 to 150 μm from the surface. These cells were within the superficial dorsal horn and assessed from slices obtained from the same spinal level of same-age mice. Unit signals were acquired with an amplifier (EX1; Dagan Corporation, Minneapolis, MN). The data were digitized with an analog-to-digital converter (Digidata 1400A; Molecular Devices, Union City, CA) stored on a personal computer with a data acquisition program (Clampex software, version 10.2; Molecular Devices) and analyzed with Clampfit software (version 10.2; Molecular Devices). We searched the area on the skin where touch (with a cotton wisp) or noxious pinch (with forceps) stimulus produced a neural response. A mechanical stimulus was applied by skin folding using a fine von Frey filament at a bending force of 255 mN. The stimuli were applied for 10 seconds to the ipsilateral hind limb at the maximal response point of the respective receptive area.

2.7. Isolation of mouse dorsal root ganglion neurons

After anesthesia with isoflurane, the dorsal root ganglion (DRG) was separated from the L4 to L6 of mice after perfusion with 10 mL ice-cold artificial cerebrospinal fluid (aCSF: 124 mM NaCl, 5 mM KCl, 1.2 mM KH_2PO_4, 1.3 mM $MgSO_4$, 2.4 mM $CaCl_2$, 10 mM glucose, 24 mM $NaHCO_3$, and equilibrated with 95% O_2 and 5% CO_2 for 1 hour on ice). The tissues were incubated with 725 μg of collagenase type IX (lot# SLBG3258; Sigma-Aldrich) in 250 μL of Earle's balanced salt solution (Sigma-Aldrich) containing 10% FBS (as above), MEM vitamin solution (1:100, Sigma-Aldrich), penicillin-streptomycin (1:200, Life Technologies, Carlsbad, CA), and GlutaMax (1:100, Life Technologies) at 37°C for 25 minutes. Next, the DRG neurons were mechanically separated by 10 to 20 cycles of pipetting using a small diameter Pasteur pipette and filtered through a 40-μm cell strainer (BD Falcon, Franklin Lakes, NJ). The isolated neurons were placed on 12-mm diameter coverslips (Matsunami, Japan) with 40 μL of aCSF and used for experiments within 4 hours after isolation, maintaining them at 37°C in a 95% O_2 and 5% CO_2 humidified chamber.

2.8. Calcium imaging and electrophysiology

Both calcium imaging and whole-cell patch-clamp recording experiments were performed 18 to 30 hours after transfection in the case with HEK293T cells. The extracellular standard bath solution contained 140 mM NaCl, 5 mM KCl, 2 mM $MgCl_2$, 2 mM $CaCl_2$, 10 mM HEPES, and 10 mM glucose at pH 7.4, adjusted with NaOH. For patch-clamp recordings, $CaCl_2$ was omitted to avoid channels desensitization. Cytosolic-free Ca^{2+} concentrations were measured with Fura-2 (Molecular Probes, Invitrogen Corp). Fura-2-AM (5 μM) was loaded 1 hour before recording, and it was excited at 340/380 nm with emission at 510 nm. Fura-2

fluorescence was recorded with a CCD camera, CoolSnap ES (Roper Scientific/Photometrics, Sarasota, FL). Data were acquired using imaging processing software IPlab (Solution Systems, Funabashi, Japan) and analyzed with ImageJ (NIH). The population of capsaicin-sensitive or AITC-sensitive neurons was determined by the number of neurons responding to capsaicin or AITC divided by the number of neurons responding to ionomycin and expressed in percentage. For whole-cell patch-clamp recording, the intracellular pipette solution contained 140 mM KCl, 5 mM EGTA, and 10 mM HEPES at pH 7.4 adjusted with KOH. Recording started 2 to 3 minutes after making a whole-cell configuration to achieve steady state. The data from whole-cell patch-clamp recordings were acquired at 10 kHz and filtered at 5 kHz for analysis (Axopatch 200B amplifier with pCLAMP software, Molecular Devices). Membrane potential was clamped at 0 or −60 mV, and voltage ramp pulses from −100 to +100 mV (300 ms) were applied every 5 seconds.

2.9. Pain-related behavior test

Mice were twice handled gently for 20 minutes at 48 and 24 hours before the behavior test. Mice were injected with capsaicin or AITC with or without diluted mosquito head homogenates or sialorphin (total 10 μL) into the top of the hind paw using a fine needle (30 G) filled with saline (Otsuka Pharmaceutical, Tokyo, Japan) containing 0.3% ethanol (capsaicin or AITC was dissolved in 0.3% ethanol). Mice were gently wrapped in the measurer's hand and injected in this position. Mice were still very quiet during injection in this position. Their behaviors were recorded using a digital camera (P6000, Nikon, Tokyo, Japan) and analyzed later.

2.10. Statistical analysis

Data are presented as means ± SEM. Statistical analysis was performed by one-way analysis of variance (with Bonferroni correction) or an unpaired Student t-test. $P < 0.05$ was considered to be significant. Statistical significance is defined as: *$P < 0.05$; **$P < 0.01$ and ***$P < 0.001$.

3. Results

3.1. Inhibition of transient receptor potential vanilloid 1–mediated and transient receptor potential ankyrin 1–mediated currents by mosquito head homogenates or mouse saliva

To determine whether mosquito saliva contains antinociceptive substances that could contribute to their painless piercings, we first evaluated the effect of mosquito head homogenates instead of mosquito saliva in rat spinal cord neurons on mechanical stimulation because we needed large amounts of mosquito saliva. In the second layer of spinal dorsal horn neurons, von Frey filament (26 g)–evoked firing frequencies were significantly reduced on injection of 0.5% lidocaine or a 10-fold dilution of mosquito head homogenates (13.2 ± 1.9 Hz, 1.9 ± 0.4 Hz, and 7.8 ± 1.5 Hz for control, lidocaine, and mosquito head homogenates, respectively; **Figs. 1B and C**), suggesting an antinociceptive effect of mosquito saliva. Then, we investigated the effects of mosquito head homogenates on TRP channel function, focusing on human TRPV1 and human TRPA1 expressed heterologously in HEK293T cells. We held the membrane potential at 0 mV and applied voltage ramp pulses from −100 to +100 mV every 5 seconds for the recording of TRPV1 currents. Diluted samples from mosquito heads
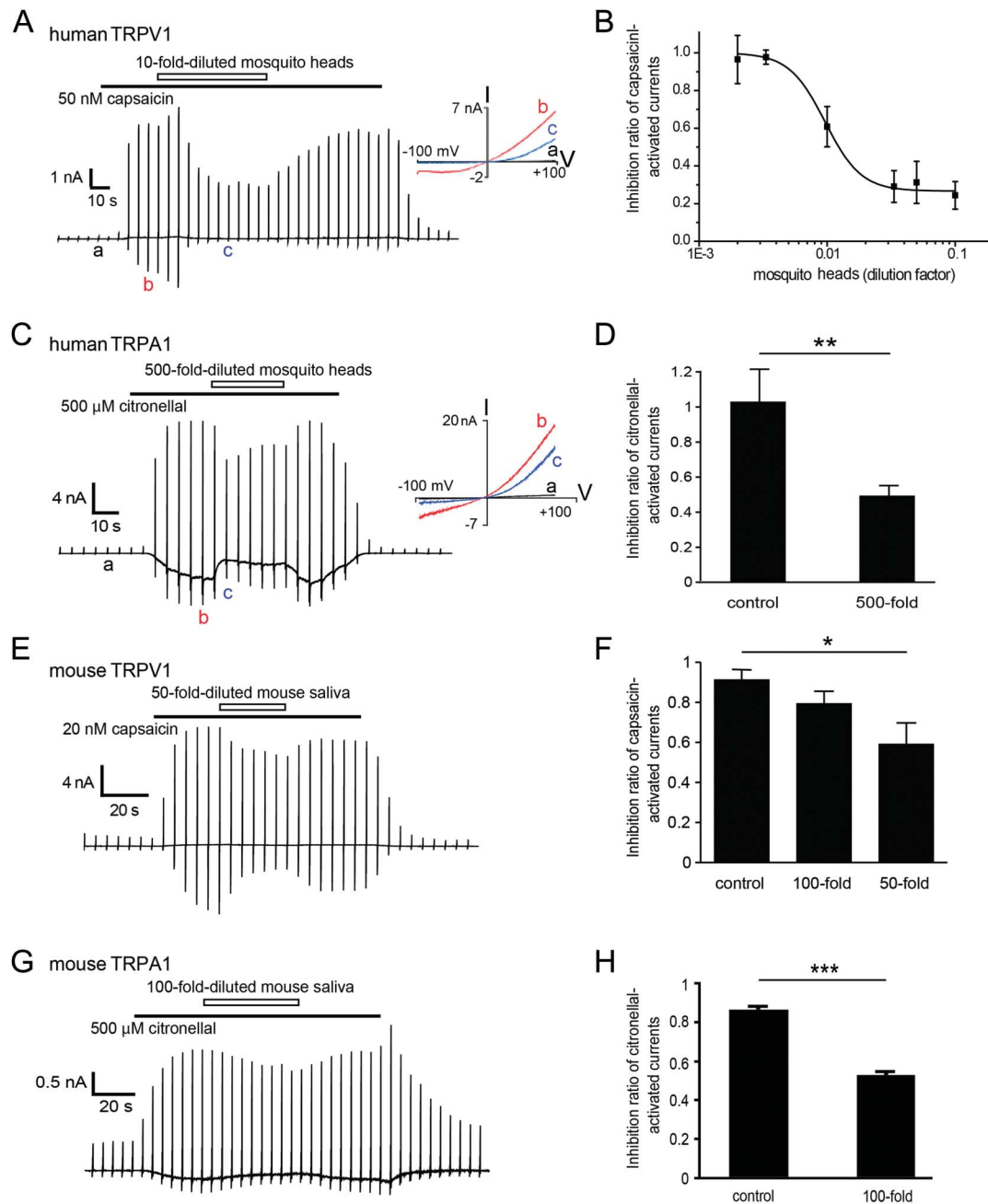
Figure 2. Inhibition of TRPV1-mediated and TRPA1-mediated currents by mosquito head homogenates or mouse saliva. (A) Representative trace of inhibition of capsaicin (50 nM)–activated human TRPV1 currents by a 10-fold dilution of mosquito head homogenates. Holding potential was 0 mV with ramp pulses ($-100 \sim$ $+100$ mV, 300 ms) applied every 5 seconds. (inset) The current–voltage (I–V) curve at the points indicated by a, b, and c in the trace. (B) The dose-inhibition curve of capsaicin (50 nM)–evoked currents at -60 mV in the presence of mosquito head homogenates at different dilution factors. Data are presented as the inhibition ratio that is the current amplitudes before application of head homogenates divided by the current amplitudes after application and normalized to the ratio of control currents (before and after saline application) at the same time points. (n = 7, 6, 7, 7, 6, 5, and 5 cells for control, 500-fold, 300-fold, 100-fold, 30-fold, 20-fold, and 10-fold dilution, respectively). (C) Representative trace of inhibition of citronellal (500 μM)–activated human TRPA1 currents by a 500-fold dilution of mosquito head homogenates. Holding potential was -60 mV with ramp pulses ($-100 \sim +100$ mV, 300 ms) applied every 5 seconds. (inset) The I–V curve at the points indicated by a, b, and c in the trace. (D) Comparison of the citronellal (500 μM)–evoked currents at -60 mV in the presence of saline (control) or mosquito head homogenates at 500-fold dilution. Data are presented as the inhibition ratio that is the current amplitudes before application of head homogenates divided by the current amplitudes after application and normalized to the ratio of control currents (before and after saline application) at the same time points. **$P < 0.01$ by the Student t test (n = 9 cells for control and n = 9 cells for 500-fold dilution). (E) Representative trace of inhibition of capsaicin (20 nM)–activated mouse TRPV1 currents by a 50-fold dilution of mouse saliva. Holding potential was 0 mV with ramp pulses ($-100 \sim +100$ mV, 300 ms) applied every 5 seconds. (F) Comparison of capsaicin (50 nM)–evoked currents at -60 mV in the presence of saline (control) or mouse saliva at different dilution factors. Data are presented as the inhibition ratio that is the current amplitudes before application of saliva divided by the current amplitudes after application and normalized to the ratio of control currents (before and after saline application) at the same time points. *$P < 0.05$ by one-way ANOVA followed by a Bonferroni post hoc test (n = 10, 5, and 9 cells for control, 100-fold and 50-fold dilution, respectively). (G) Representative trace of inhibition of citronellal (500 μM)–activated mouse TRPA1 currents by a 100-fold dilution of mouse saliva. Holding potential was -60 mV with ramp pulses ($-100 \sim +100$ mV, 300 ms) applied every 5 seconds. (H) Comparison of citronellal (500 μM)–evoked currents at -60 mV in the presence of saline (control) or mouse saliva at 100-fold dilution. Data are presented as the inhibition ratio that is the current amplitudes before application of saliva divided by the current amplitudes after application and normalized to the ratio of control currents (before and after saline application) at the same time points. ***$P < 0.001$ by the Student t test (n = 5 cells for control and n = 6 cells for 100-fold dilution). ANOVA, analysis of variance; TRPA1, transient receptor potential ankyrin 1; TRPV1, transient receptor potential vanilloid 1.

significantly inhibited the human TRPV1 currents activated by 50 nM capsaicin in a reversible manner without apparent voltage dependency as observed in the current–voltage (I–V) curves (**Fig. 2A**). The inhibition was dose-dependent, with a maximum inhibition of 77% for a 10-fold dilution, and the observed IC_{50} value was a dilution factor of 0.00965 ± 0.0009, corresponding to a 103-fold dilution of mosquito head homogenates (**Fig. 2B**). Furthermore, we examined the effects of mosquito head homogenates on the human TRPA1 channel in which we used citronellal as an agonist because the currents activated by allyl isothiocyanate (AITC) or cinnamaldehyde were hardly stabilized. By holding the membrane potential at -60 mV, we applied voltage ramp pulses similar to the ones for TRPV1 current measurement. Mosquito head homogenates also inhibited human TRPA1 currents activated by 500 μM citronellal in a reversible manner without apparent voltage dependency observed in the I–V curves (**Fig. 2C**). The action of mosquito head homogenates seemed more potent on human TRPA1 than on human TRPV1 because the application of 500-fold–diluted mosquito head homogenates was already sufficient to reach an inhibition of 50.6% of human TRPA1 (**Fig. 2D**). To evaluate whether these effects of mosquito heads with salivary glands are common to other animals, we also examined the effects of mouse saliva on mouse TRPV1 and TRPA1 channels. Similar to the mosquito head homogenates, a 50-fold dilution of mouse saliva significantly inhibited mouse TRPV1-mediated current responses activated by capsaicin (20 nM) (91.4 ± 4.9 and $59.3 \pm 10.4\%$ of the values before application in control and

saliva, respectively, $P < 0.05$), whereas a 100-fold dilution significantly inhibited TRPA1-mediated current responses by citronellal (500 μM) (86.5 ± 2.6 and $53.0 \pm 2.8\%$ of the values before application in control and saliva, respectively) (**Figs. 2E–H**). Thus, the inhibition of mouse TRPA1 by mouse saliva was greater than the inhibition of mouse TRPV1 by mouse saliva, similar to the action of mosquito head homogenates on human TRPV1 and TRPA1. Similar effects on TRPV1-mediated or TRPA1-mediated currents between mosquito head homogenates and mouse saliva suggest that the effects of mosquito head homogenates are caused by mosquito saliva.

3.2. Peptides mediate transient receptor potential vanilloid 1–inhibiting effects of mosquito head homogenates

We then sought to determine the nature of the substances found in saliva that have the ability to inhibit TRPV1 and TRPA1. Because saliva contains many peptides that can constitute active substances, we used thermal degradation to broadly inactivate peptides and investigate their involvement. Heat treatment of mosquito head homogenates at 95°C for 20 minutes caused a significant loss of the TRPV1-inhibiting effects, whereas treatment at 95°C for 5 minutes showed only a slight decrease of these inhibiting effects ($30.6 \pm 10.9\%$, $50.7 \pm 7.7\%$, and $83.3 \pm 7.5\%$ of the values before application for 0, 5, and 20 minutes treatments, respectively; **Figs. 3A–C**). Heat treatment (20 minutes) also suppressed the inhibition of capsaicin (50 nM)–
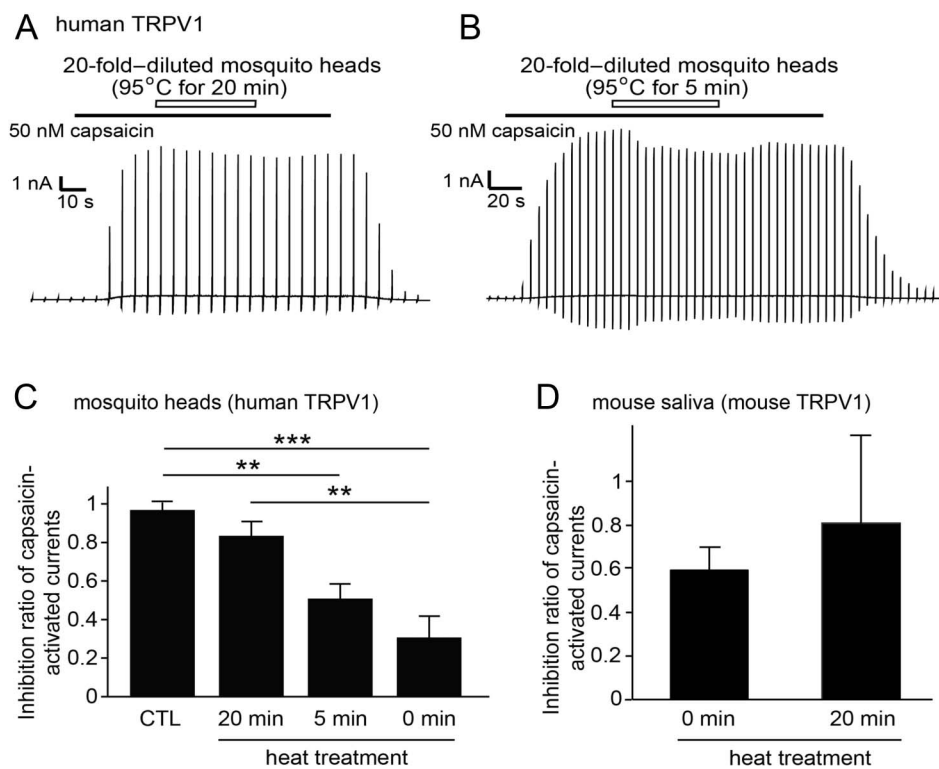

Figure 3. Loss of inhibition of TRPV1 currents by heated mosquito head homogenates. (A and B) Representative traces of inhibition of the capsaicin (50 nM)–activated human TRPV1 currents by a 20-fold dilution of mosquito head homogenates treated for 20 (A) or 5 (B) minutes with 95°C heat. Holding potential was 0 mV with ramp pulses ($-100 \sim +100$ mV, 300 ms) applied every 5 seconds. (C) Comparison of capsaicin (50 nM)–evoked currents at -60 mV in the presence of saline (control) or heat-treated mosquito head homogenates for 20, 5, or 0 minutes. Data are presented as the inhibition ratio that is the current amplitudes before application of head homogenates divided by the current amplitudes after application and normalized to the ratio of control currents (before and after saline application) at the same time points. *$P < 0.05$, **$P < 0.01$ by one-way ANOVA followed by a Bonferroni post hoc test ($n = 8$, 6, 7, and 5 cells for control, 20-fold–diluted mosquito saliva with 20, 5, or 0 minutes heat treatment, respectively). (D) Comparison of capsaicin (20 nM)–activated mouse TRPV1 currents at -60 mV in the presence of heat (95°C)–treated mouse saliva for 0 or 20 minutes. Data are presented as the inhibition ratio that is the current amplitudes before application of saliva divided by the current amplitudes after application and normalized to the ratio of control currents at the same time points. ($n = 9$ and 8 cells for 50-fold–diluted mouse saliva with 0 and 20 minutes heat treatment, respectively). ANOVA, analysis of variance; TRPA1, transient receptor potential ankyrin 1; TRPV1, transient receptor potential vanilloid 1.

activated mouse TRPV1 currents by mouse saliva, although it was not statistically significant (**Fig. 3D**). These results suggest the involvement of peptides in the antinociceptive effects of mosquito heads with salivary glands.

3.3. Inhibition of human transient receptor potential vanilloid 1–mediated and transient receptor potential ankyrin 1–mediated currents by sialorphin

To narrow down our investigation, we checked the current literature for peptides exhibiting analgesic properties and that are present in saliva. Interestingly, the endopeptidase sialorphin (**Fig. 4A**), found in rat saliva, was shown to have antinociceptive effects when applied in vivo in rat.[11] Accordingly, we examined the effects of sialorphin on TRP channel functions. Sialorphin significantly inhibited human TRPV1-mediated and TRPA1-mediated currents in a dose-dependent and reversible manner with observed IC_{50} values of 1.9 ± 0.0 μM and 4.1 ± 0.4 μM, respectively (**Figs. 4B–E**), in a similar way to what we observed for both mosquito head homogenates and mouse saliva. Although the IC_{50} value was a little bit lower for TRPV1, the maximal level of inhibition of TRPV1 channels was only of $21.7 \pm 0.1\%$, whereas it reached an inhibition of $72.8 \pm 2.8\%$ of TRPA1 channels, suggesting that sialorphin also exhibits a more potent inhibition effect on TRPA1 channels. Surprisingly, heated sialorphin rather increased the capsaicin-activated currents, (**Fig. 4F**) whereas nonheated sialorphin inhibited the currents. Then, we evaluated the antinociceptive properties of sialorphin in the spinal cord assay (**Fig. 4G**). We observed a significant reduction in von Frey filament (26 g)–evoked firing frequencies on injection of sialorphin (14.3 ± 2.3, 14.1 ± 2.2, and 6.7 ± 1.2 Hz for control, saline, and sialorphin, respectively, $P < 0.05$). These results implicate sialorphin as a strong candidate for causing the antinociceptive effects of saliva.

3.4. Mosquito head homogenate–induced inhibition of transient receptor potential vanilloid 1–mediated or transient receptor potential ankyrin 1–mediated responses in mouse DRG neurons

We next aimed to determine whether similar inhibition could be observed in mice sensory neurons. Mosquito head homogenates diluted 10-fold inhibited the capsaicin-activated currents (an inhibition of $51.5 \pm 0.5\%$) in native sensory neurons from mouse dorsal root ganglia (DRG), which consist of different peripheral sensory neurons including the ones that express TRPV1 or TRPA1[16] (**Fig. 5A**). The capsaicin-induced increase in intracellular Ca^{2+} concentrations ($[Ca^{2+}]_i$) was also slightly reduced by a 20-fold dilution of mosquito head homogenates, although this difference was not statistically significant (**Fig. 5B**). However, the population of capsaicin-sensitive neurons was significantly smaller in the presence of a 20-fold dilution of mosquito head homogenates. Surprisingly, sialorphin (3 μM) rather enhanced the capsaicin-induced $[Ca^{2+}]_i$ increase similar to the results with the heated sialorohin in the patch-clamp experiments (**Fig. 4F**), suggesting some interaction occurring between the 2 compounds. By contrast, a 20-fold dilution of mosquito head homogenates significantly inhibited the AITC (300 μM)–induced $[Ca^{2+}]_i$ increase, although the population of AITC-sensitive neurons was not modulated (**Fig. 5C**). On the other hand, sialorphin (10 μM) did not alter the AITC (300 μM)–induced $[Ca^{2+}]_i$ increase and neither amplified the response to AITC, suggesting that the phenomenon observed for capsaicin is specific for this compound. All together these results indicate a potential inhibitory effect of saliva on TRPV1 and TRPA1 in sensory neurons, whereas sialorphin effects could not be deduced with the experimental settings used.

3.5. Mosquito head homogenate–induced inhibition of capsaicin-induced or allyl isothiocyanate–induced pain-related behaviors in mice

To confirm the antinociceptive effects of saliva and sialorphin in vivo, we evaluated pain-related licking behaviors in mice for 5 minutes after injection of 10 μL of 1 μM capsaicin or 10 μL of 100 mM AITC into their hind paw. Coinjection with either mosquito head homogenates (10 μL of 2-fold–diluted samples) or sialorphin (10 μL of a 10 μM solution) into the hind paws of mice caused a reduction in licking behaviors compared with saline (**Figs. 5D and E**), indicating that both mosquito head samples with salivary glands and sialorphin have antinociceptive properties in vivo.

4. Discussion

From the data presented above, we conclude that mosquito head homogenates containing saliva and mouse saliva exhibit antinociceptive effects through the inhibition of TRPV1 and TRPA1 channels and that sialorphin could be a candidate substance contained in saliva that may cause these effects. In the case of mosquito, we cannot exclude the possibility that something else in the heads other than saliva causes this effect because we did not isolate mosquito saliva. In addition, other substances than sialorphin could be involved in the observed nociception through the inhibition of TRPV1 or TRPA1 as well. Mosquitoes seem to use this saliva-induced inhibition of TRPV1 and TRPA1 and skillful movement of their thin fascicle in concert to effectively enable painless piercing. Given the results that both mosquito heads with salivary glands and mouse saliva showed similar inhibitory effects on TRPV1 and TRPA1, this suggests that the antinociceptive properties of saliva are universal, which could explain why many animals including humans often lick their wounds.

On mosquito piercing, TRPV1 and TRPA1 channels might be activated mechanically. Although the mechanical sensitivity of these 2 channels has been recently disputed,[10] several studies reported their activation by different types of mechanical stimulation in different cell models.[1,3,4,9,13] It is difficult to estimate whether mosquito piercing would be sufficient to activate TRPV1 and TRPA1 by itself, but it is also possible that another mechanism accompanies or enhances the mechanical stimulation.

Mosquito head homogenates and mouse saliva showed a strong inhibition of TRPV1 and TRPA1 in patch-clamp recordings of HEK293T cells and mouse DRG neurons (**Figs. 2 and 5A**) but a somewhat weaker effect in $[Ca^{2+}]_i$ changes in mouse DRG neurons (**Figs. 5B and C**). In Ca^{2+} imaging recordings, the concomitant application of capsaicin or AITC with saliva might not be very efficient in blocking the Ca^{2+} influx through the channel, as evidenced by a significant delay but not a complete inhibition of the AITC-evoked $[Ca^{2+}]_i$ increase as shown in **Figure 5C**. The concentration of saliva or mosquito head homogenates used in Ca^{2+} imaging experiments of DRG neurons might also have been insufficient to reach a high blockade of $[Ca^{2+}]_i$ changes. Nonetheless, mosquito head homogenates induced a significant decrease in pain-related behaviors in mice (**Figs. 5D and E**), supporting the antinociceptive action of mosquito saliva through TRPV1 and TRPA1 channels.
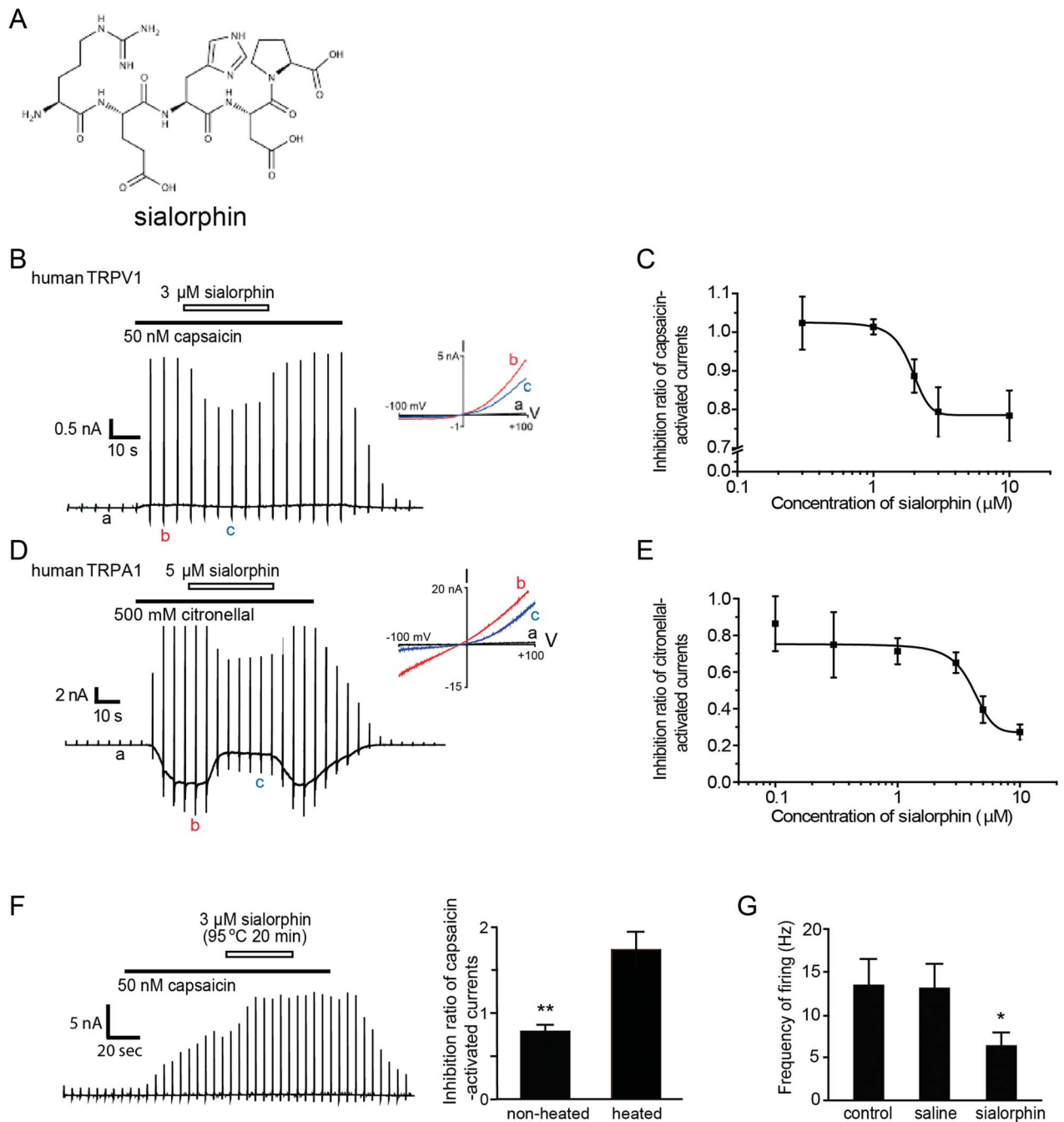
Figure 4. Inhibition of human TRPV1-mediated and TRPA1-mediated currents by sialorphin. (A) Structure of sialorphin. (B) Representative trace of inhibition of capsaicin (50 nM)–activated human TRPV1 currents by sialorphin (3 μM). Holding potential was 0 mV with ramp pulses ($-100 \sim +100$ mV, 300 ms) applied every 5 seconds. (inset) The I–V curve at the points indicated by a, b and c in the trace. (C) The dose-inhibition curve of capsaicin (50 nM)–evoked currents at -60 mV in the presence of sialorphin at different concentrations. Data are presented as the inhibition ratio that is the current amplitudes before application of sialorphin divided by the current amplitudes after application and normalized to the ratio of control currents (before and after saline application) at the same time points. (n = 8, 6, 7, 7, 10, and 5 cells for control and 0.3, 1, 2, 3, and 10 μM sialorphin, respectively). (D) Representative trace of inhibition of citronellal (500 μM)–activated human TRPA1 currents by sialorphin (5 μM). Holding potential was -60 mV with ramp pulses ($-100 \sim +100$ mV, 300 ms) applied every 5 seconds. (inset) The I–V curve at the points indicated by a, b, and c in the trace. (E) The dose-inhibition curve of capsaicin (50 nM)–evoked currents at -60 mV in the presence of sialorphin at different concentrations. Data are presented as the inhibition ratio that is the current amplitudes before application of sialorphin divided by the current amplitudes after application and normalized to the ratio of control currents (before and after saline application) at the same time points. (n = 7, 5, 6, 7, 7, 7, and 5 cells for control and 0.1, 0.3, 1, 3, 5, and 10 μM sialorphin, respectively). (F) Left, representative trace of the effect of heat-treated (95°C for 20 minutes) sialorphin (3 μM) on capsaicin (50 nM)–activated human TRPV1 currents. Holding potential was 0 mV with ramp pulses ($-100 \sim +100$ mV, 300 ms) applied every 5 seconds. Right, comparison of capsaicin (50 nM)–evoked currents at -60 mV in the presence of heat-treated sialorphin for 0 or 20 minutes. Data are presented as the inhibition ratio that is the current amplitudes before application of saliva divided by the current amplitudes after application and normalized to the ratio of control currents (before and after saline application) at the same time points. ** $P < 0.01$ by the Student t test (n = 8 and 6 cells for 0 and 20 minutes heat treatment, respectively). (G) Inhibition of vFF-evoked neuronal firing frequency in rat spinal dorsal horn neurons by 3 μM sialorphin. * $P < 0.05$ by one-way ANOVA followed by a Bonferroni post hoc test (n = 8 rats for each group). ANOVA, analysis of variance; TRPA1, transient receptor potential ankyrin 1; TRPV1, transient receptor potential vanilloid 1.
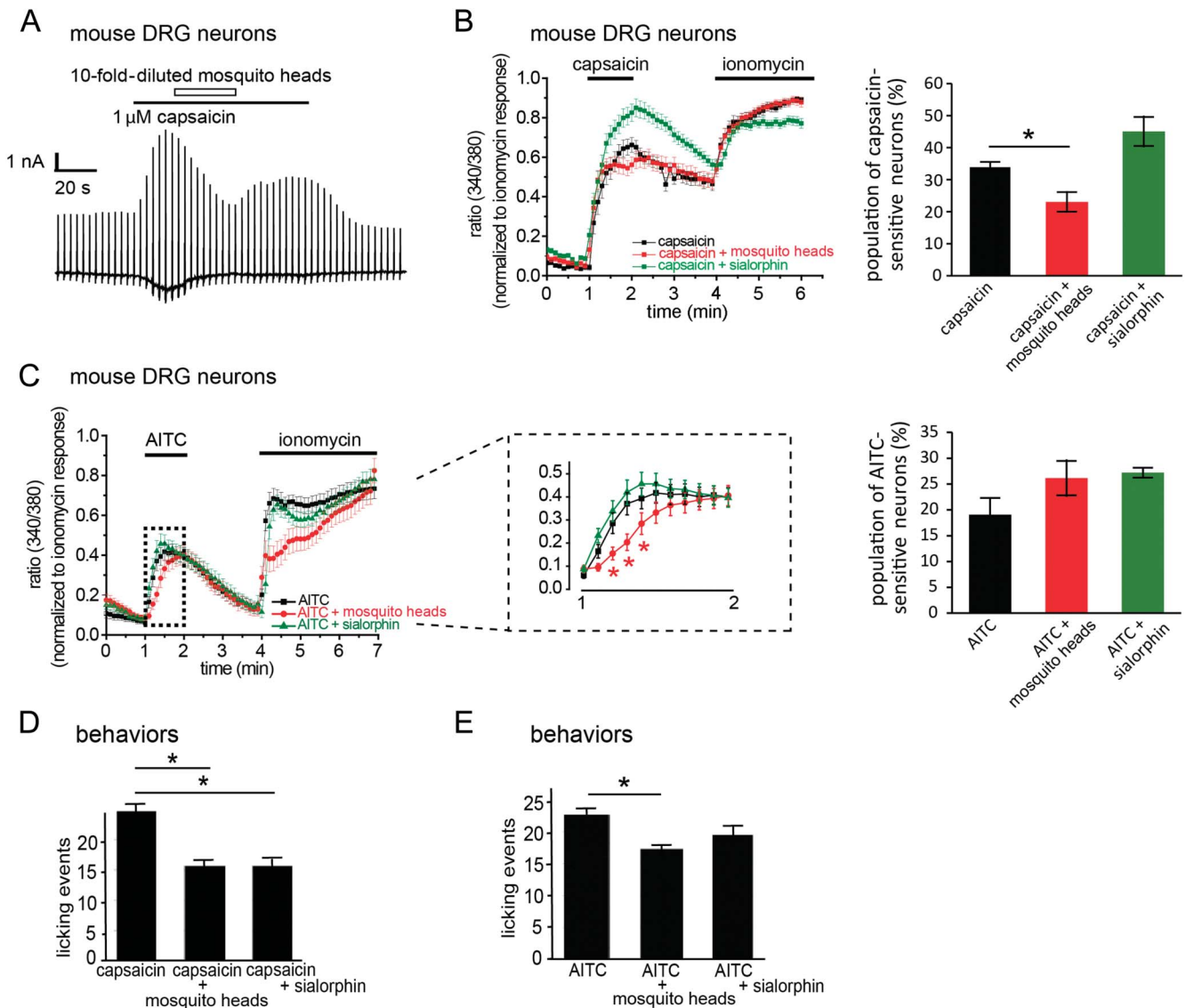
Figure 5. Inhibition of TRPV1-mediated or TRPA1-mediated responses in mouse DRG neurons and pain-related behaviors in mice by mosquito head homogenates or sialorphin. (A) Representative trace of inhibition of capsaicin (1 μM)–activated currents by a 10-fold dilution of mosquito head homogenates in a mouse DRG neuron. Similar results were observed in 3 additional cells. Holding potential was -60 mV with ramp pulses ($-100 \sim +100$ mV, 300 ms) applied every 3 seconds. (B) Left, mean changes in Fura-2 ratios in mouse DRG neurons exposed to capsaicin (50 nM) + saline (n = 32, black), + 20-fold–diluted mosquito head homogenates (n = 26 cells, red), or + sialorphin (3 μM, n = 67 cells, green), respectively. Right, comparison of the population of capsaicin-sensitive neurons (n = 140, 170, and 164 cells for saline, mosquito head homogenates, and sialorphin condition, respectively). * $P < 0.05$ by one-way ANOVA followed by a Bonferroni post hoc test. (C) Left, mean changes in Fura-2 ratios in mouse DRG neurons exposed to AITC (300 μM) + saline (n = 36, black), + 20-fold–diluted mosquito head homogenates (n = 24 cells, red), or + sialorphin (10 μM, n = 30 cells, green), respectively. Inset shows enlarged traces between one and 2 minutes of the recordings. *$P < 0.05$ by the Student t test between AITC + saline and AITC + saliva. Right, comparison of the population of AITC-sensitive neurons (n = 143, 197, and 176 cells for saline, saliva, and sialorphin condition, respectively). (D) Comparison of the total licking events in mice injected with capsaicin + saline (control, 24.8 times, n = 10 mice), + 2-fold–diluted mosquito head homogenates (middle, 15.7 times, n = 11 mice), or + sialorphin (right, 15.6 times, n = 11 mice). *$P < 0.05$ by one-way ANOVA followed by a Bonferroni post hoc test. (E) Comparison of total licking events in mice injected with AITC + saline (control, 22.6 times, n = 14 mice), + 2-fold–diluted mosquito head homogenates (middle, 17.3 times, n = 15 mice), or + sialorphin (right, 19.5 times, n = 15 mice). *$P < 0.05$ by the Student t test. AITC, allyl isothiocyanate; ANOVA, analysis of variance; DRG, dorsal root ganglia; TRPA1, transient receptor potential ankyrin 1; TRPV1, transient receptor potential vanilloid 1.

Regarding sialorphin, although its inhibition of TRPV1 and TRPA1 is obvious in patch-clamp recordings in HEK293T cells (**Fig. 4**), we did not see its clear effects in patch-clamp recordings and $[Ca^{2+}]_i$ changes in mouse DRG neurons (**Figs. 5B and C**). It could be partly because a lot of TRPV1 or TRPA1 proteins are expressed in HEK293T cells, which makes it easier to see the effects. In addition, we used AITC to stimulate TRPA1 in native mouse DRG neurons and in behavior experiments (**Figs. 5C and E**) because there is no report to date on citronellal-induced pain-related behaviors, and it might account for some difference from

the results observed in HEK293T cells in which action of sialorphin was tested against citronellal. Moreover, we observed enhanced increases of capsaicin-induced $[Ca^{2+}]_i$ in mouse DRG neurons in the presence of sialorphin (**Fig. 5B**). Although we currently have no clear explanation for this result, there might be some direct interaction of sialorphin with capsaicin, but not with AITC, which could be supported by the result that capsaicin-activated currents were increased by the heated sialorphin (**Fig. 4F**). Alternatively, sialorphin could activate another pathway that ultimately enhances capsaicin-evoked $[Ca^{2+}]_i$ increase in DRG

neurons. Because a similar phenomenon was reported for the peptide endothelin-1.[18] However, this interaction or mechanism does not seem to interfere with the antinociceptive effects of sialorphin because sialorphin did reduce the licking behaviors (**Fig. 5D**). We could not exclude the possibility that substances contained in saliva other than sialorphin contribute to the saliva-induced antinociception because the reported sialorphin concentrations[12] in rat saliva are smaller than the IC_{50} values inhibiting TRPV1 or TRPA1 activities in our study.

Overall, the findings in our study show a great potential for the natural substances present in mosquito and mouse saliva, including sialorphin, in the discovery and development of novel analgesic agents.

Conflict of interest statement

The authors have no conflicts of interest to declare.

Acknowledgments

References

[1] Birder LA, Nakamura Y, Kiss S, Nealen ML, Barrick S, Kanai AJ, Wang E, Ruiz G, De Groat WC, Apodaca G, Watkins S, Caterina MJ. Altered urinary bladder function in mice lacking the vanilloid receptor TRPV1. Nat Neurosci 2002;5:856–60.

[2] Clement AN. The biology of mosquitoes. New York, NY: CABI Publishing, 2000.

[3] Fujita F, Uchida K, Takayama Y, Suzuki Y, Takaishi M, Tominaga M. Hypotonicity-induced cell swelling activates TRPA1. J Physiol Sci 2018; 68:431–40.

[4] Gevaert T, Vandepitte J, Ost D, Nilius B, De Ridder D. Autonomous contractile activity in the isolated rat bladder is modulated by a TRPV1 dependent mechanism. Neurourology and urodynamics 2007;26: 424–32. discussion 451-423.

[5] Heinemann L. Finger pricking and pain: a never ending story. J Diabetes Sci Technol 2008;2:919–21.

[6] Izumi H, Suzuki M, Aoyagi S, Kanzaki T. Realistic imitation of mosquito's proboscis: electrochemically etched sharp and jagged needles and their cooperative inserting motion. Sensor Actuat a-Phys 2011;165:115–23.

[7] Julius D. TRP channels and pain. Annu Rev Cell Dev Biol 2013;29: 355–84.

[8] Moore C, Liedtke WB. Osmomechanical-sensitive TRPV channels in mammals. In: Emir TLR, ed. Neurobiology of TRP Channels. Boca Raton, 2017. p. 85–94.

[9] Moparthi L, Zygmunt PM. Human TRPA1 is an inherently mechanosensitive bilayer-gated ion channel. Cell Calcium 2020;91: 102255.

[10] Nikolaev YA, Cox CD, Ridone P, Rohde PR, Cordero-Morales JF, Vásquez V, Laver DR, Martinac B. Mammalian TRP ion channels are insensitive to membrane stretch. J Cel Sci 2019;132:jcs238360.

[11] Rougeot C, Messaoudi M, Hermitte V, Rigault AG, Blisnick T, Dugave C, Desor D, Rougeon F. Sialorphin, a natural inhibitor of rat membrane-bound neutral endopeptidase that displays analgesic activity. P Natl Acad Sci USA 2003;100:8549–54.

[12] Rougeot C, Rosinski-Chupin I, Njamkepo E, Rougeon F. Selective processing of submandibular rat 1 protein at dibasic cleavage sites. Salivary and bloodstream secretion products. Eur J Biochem 1994;219: 765–73.

[13] Soya M, Sato M, Sobhan U, Tsumura M, Ichinohe T, Tazaki M, Shibukawa Y. Plasma membrane stretch activates transient receptor potential vanilloid and ankyrin channels in Merkel cells from hamster buccal mucosa. Cell Calcium 2014;55:208–18.

[14] Sun D, McNicol A, James AA, Peng Z. Expression of functional recombinant mosquito salivary apyrase: a potential therapeutic platelet aggregation inhibitor. Platelets 2006;17:178–84.

[15] Suzuki MTT, Aoyagi S. 3D laser lithographic fabrication of hollow microneedle mimicking mosquitos and its characterization. Int J Nanotech 2008;15:157–73.

[16] Takayama Y, Uta D, Furue H, Tominaga M. Pain-enhancing mechanism through interaction between TRPV1 and anoctamin 1 in sensory neurons. P Natl Acad Sci USA 2015;112:5213–18.

[17] Tolle MA. Mosquito-borne diseases. Curr Probl Pediatr Adolesc Health Care 2009;39:97–140.

[18] Yamamoto H, Kawamata T, Ninomiya T, Omote K, Namiki A. Endothelin-1 enhances capsaicin-evoked intracellular Ca^{2+} response via activation of endothelin a receptor in a protein kinase Cepsilon-dependent manner in dorsal root ganglion neurons. Neuroscience 2006;137:949–60.

[19] Yoshimura M, Nishi S. Blind patch-clamp recordings from substantia gelatinosa neurons in adult rat spinal cord slices: pharmacological properties of synaptic currents. Neuroscience 1993;53:519–26.